Catalysis Today 158 (2010) 452–458

Contents lists available at ScienceDirect

Catalysis Today

journal homepage: www.elsevier.com/locate/cattod

Selective catalytic reduction of NO by hydrogen over Pt/ZSM-35

Qing Yu[a], Manfred Richter[b], Fanxiao Kong[a], Landong Li[a], Guangjun Wu[a], Naijia Guan[a,*]

[a] Key Lab of Functional Polymer Materials (Nankai University, Ministry of Education), College of Chemistry, Nankai University, No. 94 Weijin Road, Tianjin 300071, PR China
[b] Leibniz Institute for Catalysis, University of Rostock, Albert-Einstein-Str. 29A, Rostock, Germany

ARTICLE INFO

Article history:
Available online 25 July 2010

Keywords:
ZSM-35
NO reduction
H_2-SCR
Platinum

ABSTRACT

The catalytic performances of platinum catalysts supported on ZSM-5, ZSM-35 and Beta are explored for the selective catalytic reduction of NO by hydrogen (H_2-SCR). 1%Pt/ZSM-35 sample exhibits the best activity and a maximum NO conversion of 80.8% can be achieved at 120 °C with N_2 selectivity of 68.5% (GHSV = 80,000/h). In situ FTIR spectra are employed to get insight into the type of surface species formed during reaction, and NH_4^+ is found to be the key intermediate in H_2-SCR. Effects of platinum loadings on the activity of Pt/ZSM-35 are further studied between 0.1 and 2.0 wt.% Pt loading. Increase of Pt loading beyond 1.0 wt.% leads to an activity decline where a loss of strong acid sites is observed. Meanwhile, XRD and TEM results illustrate an aggregation of Pt species with increasing Pt loading on ZSM-35.

1. Introduction

Selective catalytic reduction (SCR) is the most promising way for NO_x abatement in excess oxygen. During the past decades, ammonia and hydrocarbons have been used as reductants in this reaction. While the ammonia leakage and CO_2 formation lead to a demand of a clean nontoxic reductant. Hydrogen, which is an efficient reductant of NO_x and is transformed to nothing else but water, finds favor in researcher's sight. H_2-SCR in slight excess of oxygen was firstly studied by Jones et al. [1] using Pt/Al_2O_3 catalyst. High NO_x conversion was obtained at the range of 65–200 °C, while much nitrous oxide is formed in their reaction system.

Up to now, platinum seems to be the primary choice of active component for H_2-SCR reaction. Pt catalysts supported on various oxides, such as Pt/SiO_2 [2,3], Pt/Al_2O_3 [3], $Pt/TiO_2–ZrO_2$ [4], $Pt/MgO–CeO_2$ [5], $Pt/La_{0.5}Ce_{0.5}MnO_3$ [6] have been reported to exhibit high activity in H_2-SCR. Besides oxides, zeolites have also been used as supports for Pt catalysts. Satsuma et al. investigated the H_2-SCR behavior of Pt catalysts supported on several kinds of microporous zeolites, *i.e.* MFI, MOR, Beta and Y. The acidity of supports is found to be an important factor influencing both the SCR activity and N_2 selectivity [7,8].

ZSM-35 with two-dimensional channel system (10-membered rings of 4.2 × 5.4 Å and 8-membered rings of 3.5 × 4.8 Å), belongs to FER family and possesses two kinds of acid sites [9,10]. Co-FER [11–14] and Co-Pd-FER [15] have been claimed to be active and selective in CH_4-SCR. Gallium exchanged ferrierite also shows high rates for NO_x conversion when using ammonia as reductant. The authors claim that the acidity of zeolite is very important for catalytic reduction [16]. Based on the above-mentioned results, ZSM-35 zeolite is selected as support for Pt in present study concerning NO selective reduction by hydrogen.

2. Experimental

2.1. Catalysts preparation

Parent NaZSM-35 zeolite ($SiO_2/Al_2O_3 = 30$) was kindly provided by Prof. Yuan's group of Nankai University. HZSM-35 was obtained by ion exchange of calcined NaZSM-35 zeolite with aqueous solution of ammonium nitrate three times at 80 °C for 10 h, followed by drying at 70 °C overnight and calcined at 550 °C for 6 h.

X%Pt/ZSM-35, where *x* indicates the weight loading of Pt, was prepared by wet incipient impregnation method and different volumes of K_2PtCl_6 solution were used to obtain the desired Pt loading ranging from 0.1 to 2.0 wt.%. After impregnation, the samples were dried at 70 °C overnight and then calcined at 550 °C in air for 3 h. For comparison, 1%Pt/ZSM-5 and 1%Pt/Beta catalysts were also prepared with the same method using HZSM-5 ($SiO_2/Al_2O_3 = 25$) and HBeta ($SiO_2/Al_2O_3 = 25$) as supports. The exact Pt loadings in catalyst were analyzed by ICP-OES (Varian 700-ES).

2.2. Catalysts characterization

XRD patterns of samples were performed on a Bruker D8 powder diffractometer (40 kV and 40 mA) using Cu K_α ($\lambda = 1.54178$ Å) radiation from 5° to 50° with a scan speed of $2\theta = 6.0°$/min.

Transmission electron microscopy (TEM) images of samples were acquired on a Tecnai G^2 2010 S-TWIN transmission electron microscope at an accelerate voltage of 200 kV.

---

* Corresponding author.
E-mail address: guannj@nankai.edu.cn (N. Guan).

0920-5861/$ – see front matter © 2010 Elsevier B.V. All rights reserved.
doi:10.1016/j.cattod.2010.06.031

The X-ray photoelectron spectroscopy (XPS) measurements were acquired using a PHI 5300 ESCA XPS spectrometer with monochromatic Mg K_α excitation, and all the bonding energies were calibrated to the C 1s peak at 284.6 eV of the surface adventitious carbon.

Temperature-programmed desorption of ammonia experiments (NH_3-TPD) were carried out in a quartz U-shaped reactor and was monitored by on-line chemisorption analyzer (Quantachrome ChemBet 3000). 0.1 g of the sample was pretreated at 600 °C for 1 h in He flow at 30 ml/min, then cooled to 100 °C and saturated with 5%NH_3/Ar. After that, the sample was purged with helium for *ca.* 30 min to remove physical absorbed ammonia and NH_3-TPD was carried out in the range of 100–600 °C at a heating rate of 10 °C/min.

2.3. Activity test

The selective catalytic reduction of NO by hydrogen at atmospheric pressure was carried out in a fixed-bed flow microreactor. The typical reactant gas composition was NO (1000 ppm), H_2 (5000 ppm), O_2 (6.7%), and the balance He. The total flow of the inlet gas was set at 200 ml/min. A sample weight of 0.1 g was employed, corresponding to the gas hourly space velocity (GHSV) of 80,000 h^{-1}. Prior to testing, the samples were calcined in He (100 ml/min) for 30 min at 500 °C. The products were analyzed on-line using a gas chromatograph (Varian CP-3800, for H_2, N_2 and N_2O analysis) and a chemiluminescence NO_x analyzer (Ecotech EC 9841, for NO and NO_2 analysis). The results are described in terms of NO conversion, N_2 selectivity (S_{N_2}) and H_2 conversion, which are calculated on the basis of Eqs. (1)–(3):

$$\text{NO conv.} = \frac{[\text{NO}]_0 - [\text{NO}]}{[\text{NO}]_0} \times 100\% \qquad (1)$$

Table 1
The steps of in situ FTIR performed at present work.

Steps	Experiments
1	Exposuring to reaction gas mixture for 60 min at 120 °C
2	Flushing with He for 30 min
3	Increasing temperature to 140 °C in reaction gas mixture
4	Exposuring to reaction gas mixture for 60 min at 140 °C
5	Flushing with He for 30 min

$$H_2\ \text{conv.} = \frac{[H_2]_0 - [H_2]}{[H_2]_0} \times 100\% \qquad (2)$$

$$S_{N_2} = \frac{2[N_2]}{1000 \times (\text{NO conv.})} \times 100\% \qquad (3)$$

$[\text{NO}]_0$ represents the inlet NO concentration, [NO] represents the outlet NO concentration, $[H_2]_0$ represents the inlet H_2 concentration, $[H_2]$ represents the outlet H_2 concentration and $[N_2]$ represents the outlet N_2 concentration.

2.4. FTIR studies

The in situ FTIR studies were carried out using a Bruker Tensor 27 spectrometer equipped with a heatable and evacuable IR cell with CaF_2 windows, connected to a gas dosing-evacuation system. For each experiment, the self-supporting wafer of catalyst was activated at 400 °C under helium for 30 min, and then its absorption was measured at each desired temperature (coded as S_c). The IR spectra of surface species shown in the figures were obtained by subtracting S_c from each spectrum. The spectra were recorded with 2 cm^{-1} resolution and 50 scans. Table 1 described the necessary steps performed for each in situ IR study of reaction presented

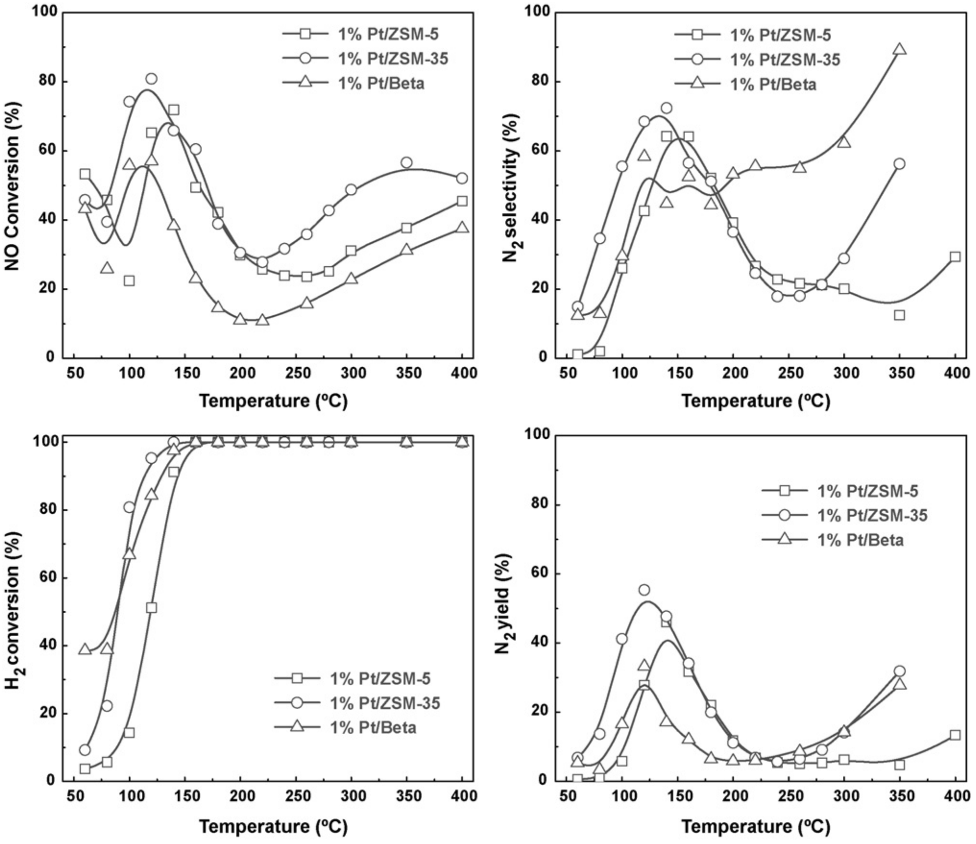

Fig. 1. Catalytic performance of 1%Pt/zeolite in H_2-SCR. Reaction conditions: 0.1% NO, 0.5% H_2, 6.7% O_2 and He balance, GHSV = 80,000 h^{-1}.

Table 2
The performance of Pt/zeolites in H_2-SCR at 120 °C.

Samples	Pt loading	NO conversion	N_2 selectivity	N_2 yield
1%Pt/ZSM-5	0.95	65.3	42.7	27.8
1%Pt/ZSM-35	0.95	80.8	68.5	55.4
1%Pt/Beta	1.04	57.1	58.3	33.3

in this work. The reaction gas mixture used is 0.1% NO, 0.5% H_2, 5% O_2 balanced with helium (100 ml/min).

3. Results and discussion

3.1. Effect of support in H_2-SCR

3.1.1. Catalytic activity of Pt/zeolites in H_2-SCR

Fig. 1 shows the catalytic performance of Pt catalysts supported on different microporous zeolites in H_2-SCR reaction. All catalysts show a maximum NO conversion in the temperature range of 100–140 °C, and starting from 200 °C, the conversion increased again with temperature. The N_2 selectivity and yield show similar trend: one peak at 100–140 °C, and another one at higher temperature. For all catalysts, H_2 was completely consumed at 160 °C. Among all catalysts studied, 1%Pt/ZSM-35 exhibits the most attractive activity in the whole temperature range. A maximum NO conversion of 80.8% can be achieved on 1%Pt/ZSM-35 at 120 °C with N_2 selectivity of 68.5%. More detailed comparison data are given in Table 2.

3.1.2. Acidity of zeolite supports and Pt/zeolites

The acidity of zeolite supports is investigated by means of NH_3-TPD and results are shown in Fig. 2. Beta, ZSM-5 and ZSM-35 all show two desorption peaks of ammonia, indicating the existence of two kinds of acid sites on these support, *i.e.* weak acid sites at temperatures lower than 300 °C and strong acid sites at temperatures higher than 400 °C. The amount of strong acid sites is observed as ZSM-5 > ZSM-35 > Beta. And the same order is observed after platinum impregnation. Besides, the peaks at high-temperature become less intense after the introduction of platinum, indicating that some of available strong acid sites are blocked by platinum.

3.1.3. In situ FTIR study on H_2-SCR

The influence of support on the H_2-SCR activity is further studied by in situ FTIR. Fig. 3 shows the surface species formed during reaction at 120 and 140 °C on different Pt/zeolites. For 1%Pt/ZSM-35, reaction at 120 °C gives bands at 1448, 1630, 2808, 3006, 3271 cm^{-1} and a negative band at 3598 cm^{-1}. The band at 1448 cm^{-1} can be assigned to NO bridged adsorption on terrace site of single crystalline Pt (112) [17] or NH_4^+ ion on Br∅nsted acid sites [8]. As this band is not observed in NO and O_2 co-adsorption, and another band corresponding to the vibration of N–H groups [18] at 3271 cm^{-1} is observed together with 1448 cm^{-1}, we assign the band at 1448 cm^{-1} to NH_4^+ ions on Br∅nsted acid sites. Bands at 1630, 2808 and 3006 cm^{-1} were assigned to molecular adsorbed water [19]. The negative band at 3598 cm^{-1} was due to the consumption of Si(OH)Al groups [20–22]. Taking account of the formation of NH_4^+ ions on Br∅nsted acid sites, it can be concluded that protons take part in the formation of ammonia ions, which agrees with the report of Satsuma et al. [8]. On the other hand, band at 1448 cm^{-1} is more intense at 120 °C than that at 140 °C, and bands corresponding to adsorbed water are less intense at 140 °C. It suggests that less NH_4^+ ions and water are formed at 140 °C. The results are consistent with the catalytic results that the activity is lower at 140 °C than that at 120 °C (Fig. 1).

For 1%Pt/ZSM-5, bands at 1349, 1448, 1630, 2476, 2808, 2900, 2993, 3255 cm^{-1} and one negative band at 3609 cm^{-1} are observed during reaction. Bands at 1448 and 3255 cm^{-1} are also assigned to NH_4^+ ions on Br∅nsted acid sites [8] and the vibration of N–H groups [18], respectively. The band at 1630 cm^{-1} is assigned to $\delta(H_2O)$ of molecular adsorbed water [18]. The observation of a negative band at 3609 cm^{-1} also suggests the consumption of Si(OH)Al groups during H_2-SCR reaction. Bands at 1349, 2900 and 2476 cm^{-1}, due to δ(OH) modes of the H-bonded zeolites hydroxyls, and the well known A-B-C structure produced by hydrogen-bonded hydroxyls [19], respectively, are clearly observed at 140 °C. Concomitantly, the intensity of bands at 1448 and 3255 cm^{-1} decreased at 140 °C. It indicated that some of the Br∅nsted acid sites occupied by NH_4^+ ions are taken by molecular water.

For 1%Pt/Beta, during H_2-SCR reaction, NH_4^+ ions (corresponding to bands at 1457 and 3217 cm^{-1}) and water (corresponding to bands at 1630, 2497, 2847 and 3041 cm^{-1}) are formed with the consumption of Si(OH)Al groups (negative band at 3600 cm^{-1} [20–22]) and terminal silanol groups (Si–OH) (negative band at 3740 cm^{-1} [18]). The intensity of bands corresponding to NH_4^+ ions and adsorbed water decreases at 140 °C, which agrees with the decreased activity (Fig. 1).

NH_4^+ ions on Br∅nsted acid sites, *e.g.* IR band at *ca.* 1450 cm^{-1} are observed as key intermediate for H_2-SCR on Pt catalysts supported on zeolites. If NO is "hydrogenated" by H_2 to NH_3, Br∅nsted acid sites of the zeolite stabilize NH_3 in form of NH_4^+ ions. The reduction of NO in excess oxygen by zeolite-fixed NH_4^+ ions is well known [23]. For different Pt/zeolite catalysts, the highest intensity of IR band corresponding to adsorbed NH_4^+ ion is observed on the sample with highest amount of strong acid sites, *i.e.* Pt/ZSM-5. For

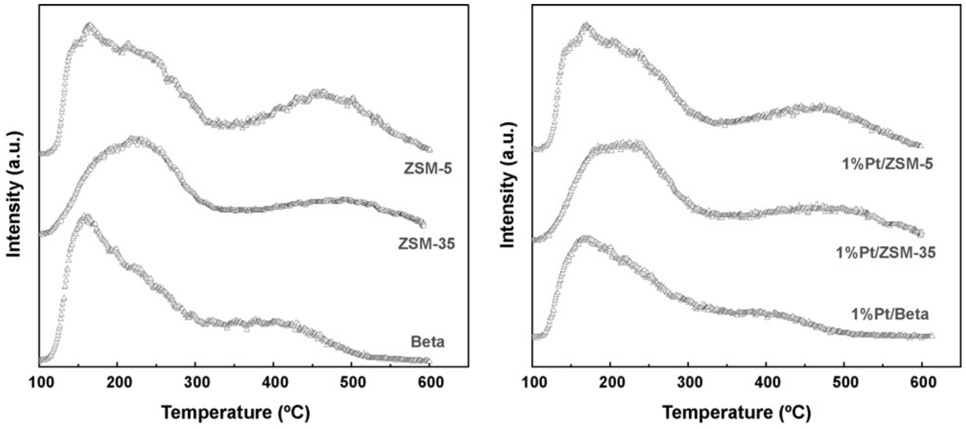

Fig. 2. NH_3-TPD profiles of zeolites and 1%Pt/zeolites.

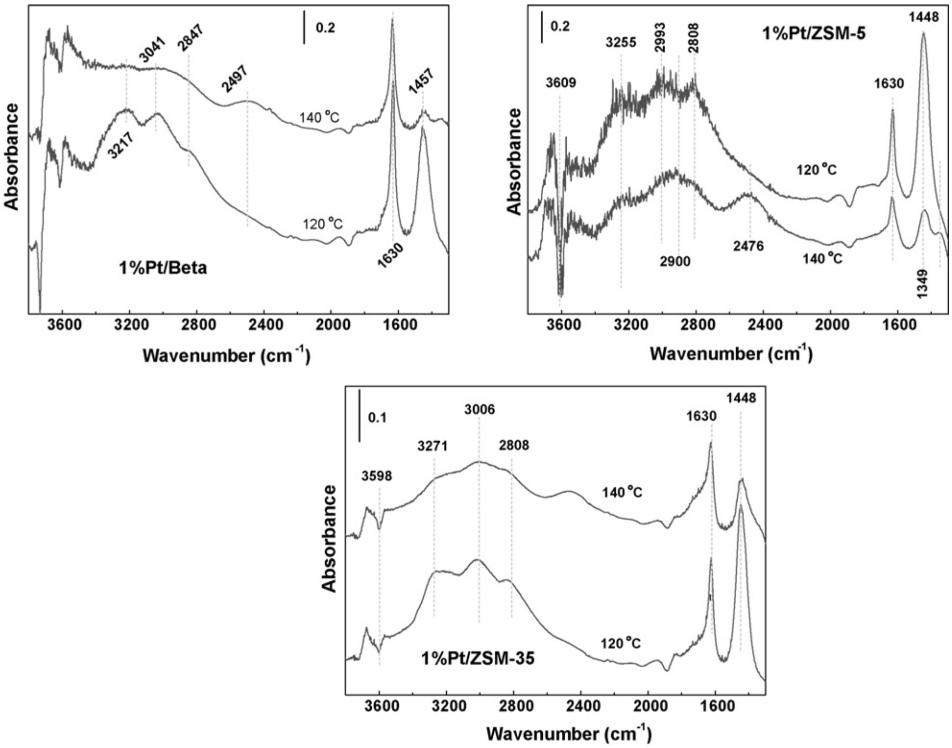

Fig. 3. FTIR spectra of surface species formed during H_2-SCR reaction on 1%Pt/zeolites. Reaction conditions: 0.1% NO, 0.5% H_2, 5% O_2 and He balance, GHSV = 80,000 h^{-1}.

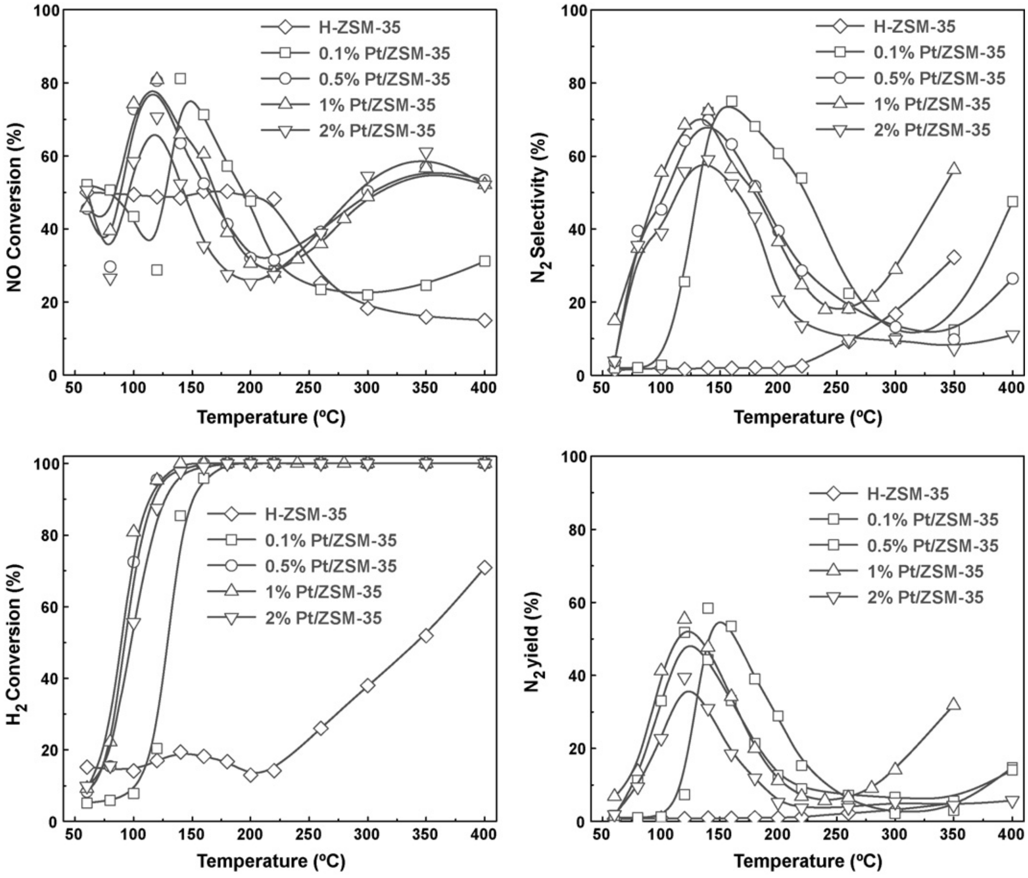

Fig. 4. Catalytic performance of *x*%Pt/ZSM-35 in H_2-SCR. Reaction conditions: 0.1% NO, 0.5% H_2, 6.7% O_2 and He balance, GHSV = 80,000 h^{-1}.

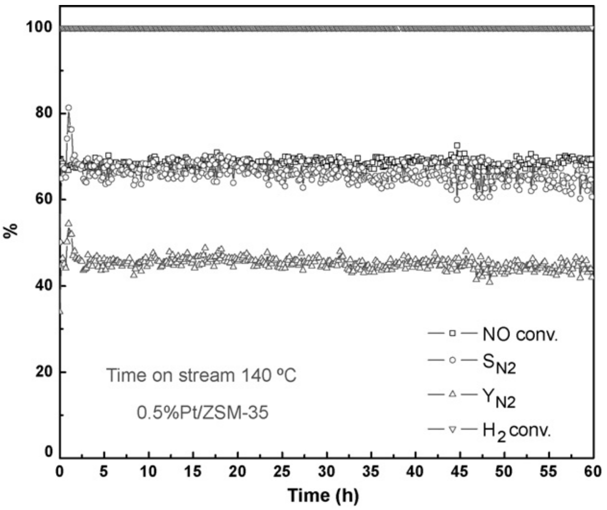

Fig. 5. Durability of 0.5%Pt/ZSM-35 catalyst in H_2-SCR. Reaction conditions: 140 °C, 1000 ppm NO, 5000 ppm H, 6.7% O, He balance, GHSV = 80,000 h^{-1}.

a given catalyst, higher H_2-SCR activity is obtained at the temperature when higher intensity of IR band corresponding to adsorbed NH_4^+ is observed. However, highest H_2-SCR activity is not observed on the catalyst with highest intensity of IR band corresponding to adsorbed NH_4^+. In this study, the good activity of Pt/ZSM-35 should, at least partially, be ascribed to the unique structure of ZSM-35. The small 8-membered pores would allow for multi-site reaction steps due to the geometry. Further research on these is in progress.

3.2. Effect of Pt loading in H_2-SCR

3.2.1. Activity of x%Pt/ZSM-35 in H_2-SCR

Taking account of the activity and selectivity, we choose Pt/ZSM-35 as promising H_2-SCR catalyst for further studies. The H_2-SCR performances of Pt/ZSM-35 catalysts with different platinum loadings are depicted in Fig. 4. Comparing with HZSM-35, incorporation of 0.1 wt.% platinum greatly increases the catalytic activity, especially the N_2 selectivity and H_2 conversion. It indicates that H_2 needs to be activated on Pt species and H_2 activation is very important for N_2 formation. With Pt loading increasing from 0.1 to 0.5 wt.%, the temperature corresponding to maximal NO conversion and N_2 selectivity shifts from 140 to 120 °C. 1%Pt/ZSM-35 exhibits quite similar performance to 0.5%Pt/ZSM-35, while 2%Pt/ZSM-35 exhibits distinct lower activity than 0.5%Pt/ZSM-35 and 1%Pt/ZSM-35.

The durability of Pt/ZSM-35 is further studied using 0.5%Pt/ZSM-35 as catalyst. As it can be seen in Fig. 5, both the activity and selectivity of catalyst can be well preserved during 60 h H_2-SCR reaction. It implies that Pt/ZSM-35 catalyst is quite stable during the reaction and has the potential for future application.

3.3. Acidity of x%Pt/ZSM-35

The influence of Pt loadings on the acidity of Pt/ZSM-35 catalysts is investigated by NH_3-TPD and the results are shown in Fig. 6. All samples exhibit two peaks of ammonia desorption: one at temperatures lower than 300 °C and another one at temperatures higher than 400 °C. HZSM-35 zeolite, used as support, possesses both weak acid sites and strong acid sites, consistent with the report of Xu and co-workers [10]. With increasing Pt loading from 0.5 to 2 wt.%, the area of high-temperature peak decreases. It suggests that some of available strong acid sites are blocked by impregnated Pt species and some of Pt species may be fixed to protonic sites. The loss of strong acid sites may be one possible reason for the low activity of 2% Pt/ZSM-35.

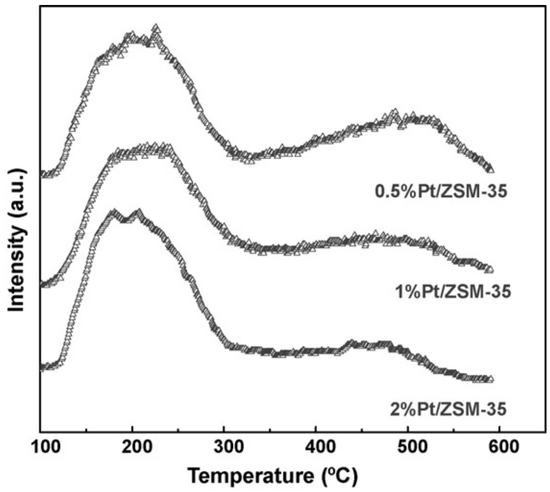

Fig. 6. NH_3-TPD profiles of x%Pt/ZSM-35.

3.4. Existence state of Pt species in x%Pt/ZSM-35

The XRD patterns of x%Pt/ZSM-35 are shown in Fig. 7. All Pt/ZSM-35 samples show diffraction patterns similar to ZSM-35 support, indicating that the framework of ZSM-35 zeolite is well preserved upon Pt impregnation. No reflections corresponding to Pt species can be observed on 0.1%Pt/ZSM-35 and 0.5%Pt/ZSM-35 catalysts. With Pt loading increasing from 0.5 to 1 wt.% and 2 wt.%, two new lines at *ca.* 39° and 46° corresponding to metallic Pt [24,25] appear. It implies that Pt species may aggregate as metal clusters with Pt loading over 1%.

TEM technique is employed to investigate the morphology of Pt species on ZSM-35 and the images are given in Fig. 8. Very few Pt particles of less than 10 nm can be found in 0.5%Pt/ZSM-35 catalyst (Fig. 8a). Comparing with 0.5%Pt/ZSM-35, much more Pt particles with larger sizes are observed on 2%Pt/ZSM-35 (Fig. 8b). The TEM observations are in well consistent with the XRD results and further confirm the aggregation of Pt species at higher Pt loadings.

The existence state of Pt in Pt/ZSM-35 is studied by means of XPS, and spectra are shown in Fig. 9. In principle, the Pt 4f and 4d core levels are both suitable for the XPS study of platinum-containing zeolites [26]. Unfortunately, the low intensity of Pt 4d line leads to

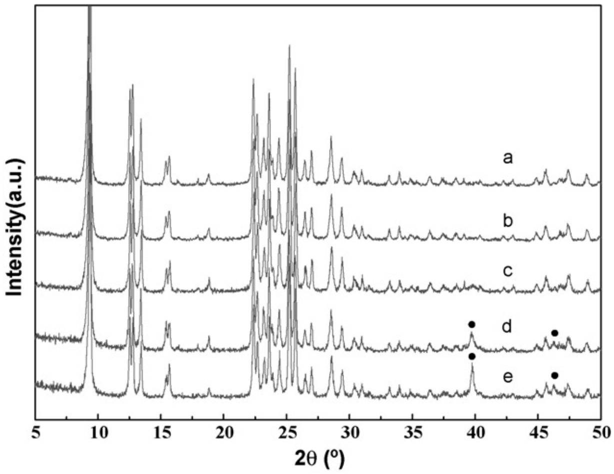

Fig. 7. XRD patterns of x%Pt/ZSM-35. x = 0 (a), x = 0.1 (b), x = 0.5 (c), x = 1 (d), x = 2 (e).

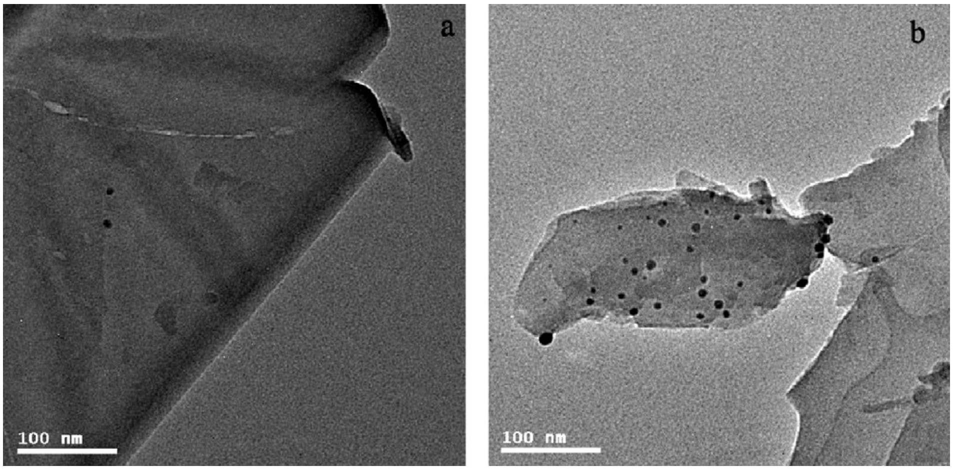

Fig. 8. TEM images of 0.5%Pt/ZSM-35 (a) and 2%Pt/ZSM-35 (b).

a decrease of analysis precision and to a limitation of minimal Pt loadings in the samples (not less than 1 wt.%). However, the Pt $4f_{5/2}$ line is overlapped by the Al 2p line (74.3 eV), and the decomposition of the Pt 4f and Al 2p profiles is made subject to the constraints of constant Pt 4f doublet separation and constant doublet intensity ratio. Pt ($4f_{7/2,\ 5/2}$) peaks in Pt/ZSM-35 catalysts are deconvoluted into two sets of spin-orbit doublet. The peaks at 70.8 and 73.6 eV are assigned to metallic Pt species while peaks at 71.8 and 74.9 eV are assigned to $Pt^{II}O$ species [24,27]. It is found that in Pt/ZSM-35 catalysts, Pt species exist mostly in Pt^0 state (80%) with the other 20% in the form $Pt^{II}O$. The Pt loadings do not influence the valence states of Pt on ZSM-35 zeolites. Since metallic Pt is known to be more active than platinum oxides, Pt/ZSM-35 exhibits quite good performance in H_2-SCR.

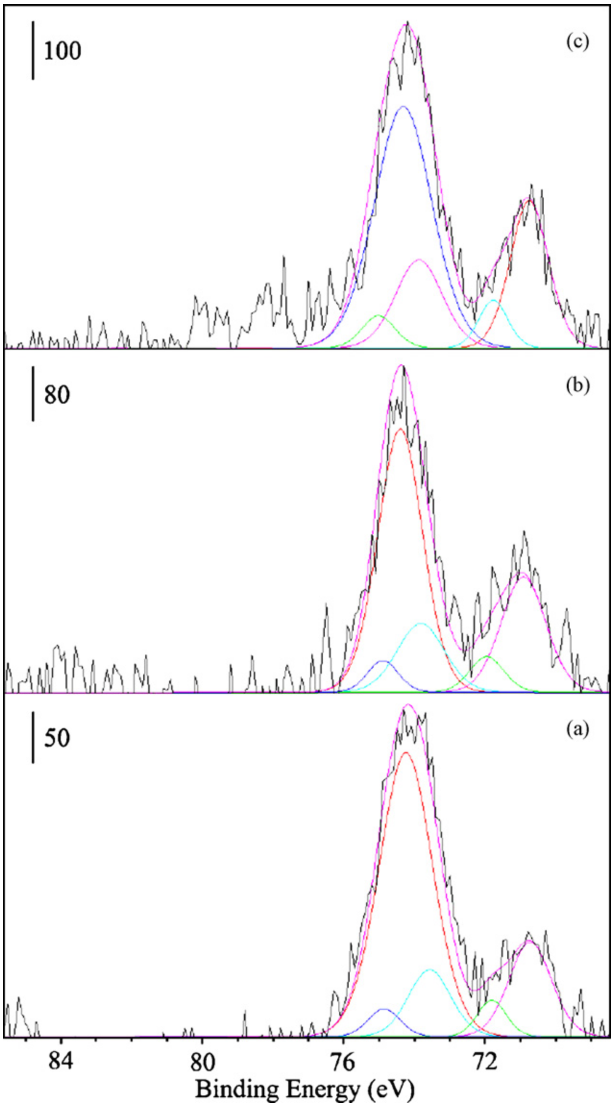

Fig. 9. XPS fitting plots of *x*%Pt/ZSM-35. *x* = 0.5 (a), *x* = 1 (b), *x* = 2 (c).

4. Conclusions

The selective catalytic reduction of NO by hydrogen in excess oxygen is investigated on Pt catalysts supported on several microporous zeolites, *e.g.* ZSM-35, ZSM-5 and Beta. With similar Pt loading of 1%, Pt/ZSM-35 exhibits the highest activity and a maximal NO conversion of 80.8% can be achieved at 120 °C with N_2 selectivity of 68.5%. In situ FTIR study reveals that NH_4^+ ions are formed during H_2-SCR reaction and they are the key intermediates involved in the reaction. The formation of NH_4^+ ions gives rise to a further activity window at higher temperatures when the reductant H_2 is completely consumed. Pt species in Pt/ZSM-35 exist mainly in the form of metallic Pt (*ca.* 80%), which is independent of Pt loadings. The H_2-SCR activity of Pt/ZSM-35 increases with Pt loading increasing from 0.1 to 1%, while declines with further increasing to 2%. The low activity in 2%Pt/ZSM-35 is ascribed to the block of acid sites and the aggregation of Pt species, as proved by XRD and TEM results.

Acknowledgements

We greatly appreciate valuable help of Dr. Ursula Bentrup at Leibniz Institute for Catalysis, University of Rostock, in FTIR measurement. This work was financially supported by International S&T Cooperation Program of China (ISCP, 2007DFA90720), PPP program and National Natural Science Foundation of China (20973094).

References

[1] J.H. Jones, J.T. Kummer, K. Otto, M. Shelef, E.E. Weaver, Environ. Sci. Technol 9 (1971) 791.
[2] R. Burch, A.A. Shestov, J.A. Sullivan, J. Catal. 188 (1999) 69.
[3] R. Burch, M.D. Coleman, J. Catal. 208 (2002) 435.
[4] M. Machida, S. Ikeda, D. Kurogi, T. Kijima, Appl. Catal. B 35 (2001) 107.
[5] C.N. Costa, P.G. Savva, J.G. Fierro, A.M. Efstathiou, Appl. Catal. B 75 (2007) 147.
[6] C.N. Costa, V.N. Stathopoulos, V.C. Belessi, A.M. Efstathiou, J. Catal. 197 (2001) 350.

[7] A. Satsuma, M. Hashimoto, J. Shibata, H. Yoshida, T. Hattori, Chem. Commun. (2003) 1698.

[8] J. Shibata, M. Hashimoto, K. Shimizu, H. Yoshida, T. Hattori, A. Satsuma, J. Phys. Chem. B 108 (2004) 18327.

[9] R. Byggningsbacka, N. Kumar, L.-E. Lindfors, J. Catal. 178 (1998) 611.

[10] S. Xie, S. Liu, Y. Liu, X. Li, W. Zhang, L. Xu, Micropor. Mesopor. Mater. 121 (2009) 166.

[11] C. Resini, T. Montanari, L. Nappi, G. Bagnasco, M. Turco, G. Busca, F. Bregani, M. Notaro, G. Rocchini, J. Catal. 214 (2003) 179.

[12] Y. Li, J.N. Armor, Appl. Catal. B (1993) L1.

[13] T.J. Lee, I. Nam, S. Ham, Y. Baek, K. Shin, Appl. Catal. B 41 (2003) 115.

[14] J. Park, C.H. Park, I. Nam, Appl. Catal. A 227 (2004) 271.

[15] A.P. Ferreira, S. Capela, P.D. Costa, C. Henriques, M.F. Ribeiro, F.R. Ribeiro, Catal. Today 119 (2007) 156.

[16] M. Mečárová, N.A. Miller, N.C. Clark, K.C. Ott, T. Pietraβ, Appl. Catal. A 282 (2005) 267.

[17] S. Chien, M. Kuo, C. Lu, K. Lu, Catal. Today 97 (2004) 121.

[18] L. Čapek, K. Novoveská, Z. Sobalík, B. Wichterlová, L. Cider, E. Jobson, Appl. Catal. B 60 (2005) 201.

[19] K. Hadjiivanov, J. Saussey, J.L. Freysz, J.C. Lavalley, Catal. Lett. 52 (1998) 103.

[20] Q. Yu, X. Wang, N. Xing, H. Yang, S. Zhang, J. Catal. 245 (2007) 124.

[21] F. Poignant, J.L. Freysz, M. Daturi, J. Saussey, Catal. Today 70 (2001) 197.

[22] L.D. Li, N.J. Guan, Micropor. Mesopor. Mater. 117 (2005) 450.

[23] M. Richter, A. Trunschke, U. Bentrup, K.W. Brzezinka, E. Schreier, M. Schneider, M.M. Pohl, R. Fricke, J. Catal. 206 (2002) 98.

[24] J. Zou, Y. Zhang, C. Liu, Langmuir 22 (2006) 11388.

[25] P. Bera, K.R. Priolkar, A. Gayen, P.R. Sarode, M.S. Hegde, S. Emura, R. Kumashiro, V. Jayaram, G.N. Subbanna, Chem. Mater. 15 (2003) 2049.

[26] J. Nováková, L. Kubelková, L. Brabec, Z. Bastl, N. Jaeger, G. Schulz-Ekloff, Zeolites 16 (1996) 173.

[27] L.D. Li, Q. Shen, J. Cheng, Z.P. Hao, Appl. Catal. B 93 (2010) 259.